ITERATED EXTENDED KALMAN FILTER WITH ADAPTIVE STATE NOISE ESTIMATION FOR ELECTRICAL IMPEDANCE TOMOGRAPHY

Flávio Celso Trigo
IMS Engenharia de Sistemas Médicos e Escola Politécnica da USP - São Paulo - Brasil
flavio.trigo@ims-eng.com

Raúl Gonzalez-Lima
Escola Politécnica da USP - São Paulo - Brasil
rauglima@usp.br

Abstract. *This work proposes and evaluates the feasibility of the iterated extended Kalman filter, incorporating an adaptive noise technique, to solve the inverse problem of Electrical Impedance Tomography. The study aims at the improvement of the method, in order to provide faster and more accurate estimates of the dielectric characteristics of a medium, mandatory requisites in medical applications. A cylindrical phantom filled with saline solution, in which a glass-object is immersed, provides experimental data used to validate the model. The immersion of the glass-object simulates a step-function perturbation on the medium. Current patterns are injected and potentials are measured through brass electrodes placed around the border of the phantom. A two-phase identification schema is employed. The approach is shown to be effective in determining the position of the glass-object and the contact impedances of the electrodes. Convergence criteria are used to assure correctness of the obtained estimates.*

Keywords: *Non-linear estimation, Kalman filters for EIT, Adaptive-noise, Model identification*

1. Introduction

Electrical Impedance Tomography (EIT) attempts to generate images of a medium from estimates of its dielectric properties. In order to accomplish this task, a low amplitude current pattern is applied to a body surface and the potential at determined points of that surface is measured through electrodes. Measured potential is a function of the conductivity/resistivity distribution and overall geometric features of the object under analysis. Since potentials are known and dielectric parameters not, the problem of estimating those properties of the medium is inverse. The conductivities/resistivities are, thus, the parameters of a model of the object; they result from the solution of the Laplace partial derivatives equation with proper boundary conditions, which governs the phenomenon.

The potential applications of EIT in Medicine range from monitoring cyclic changes in lung condition of patients in intensive care units to fast imaging of cerebrovascular accident (brain stroke); recent researches seek to use thorax images from EIT to infer blood flow through the lungs. Nowadays, lung function monitoring is the main research area among the EIT scientific community. The pursuit for methods capable of providing reliable and fast estimates of the conductivity/resistivity distribution in the medium has led to approaches that describe the inverse problem in dynamical form using a state-space approach (Vauhkonen, Karjalainen and Kaipio, 1998), in which the state-vector contains dielectric parameters to be estimated through the linearized Kalman filter. Further on, the same state-space model was used with the extended Kalman filter (Kim *et al.*, 2001; Kim *et al.*, 2002; Trigo, 2001; Trigo *et al.*, 2004).

In this work, we propose a two-phase method to solve the EIT problem based on a state-space approach to estimate time-varying absolute conductivity/resistivity in a phantom and electrode contact impedances, using the extended iterated Kalman filter as the estimator. The two-phase method characterizes by isolating estimation of medium parameters from electrode contact parameters. This approach helps minimizing numerical errors that arise from the ill-posed feature of the inverse problem.

2. Theoretical basis

2.1 Domain and Electrode Model

When a plane closed domain Γ with stationary charge and conductivity distribution $\sigma(x, y)$, and purely conductive medium is submitted to crossing steady current (Barber and Brown, 1984), the inner electrical potential Ψ is given by Laplace equation

$$\nabla.(\sigma \nabla \Psi) = 0. \tag{1}$$

At the boundary, currents are injected through electrodes; thus

$$\left[\begin{array}{ll} \sigma \frac{\partial \Psi(\sigma)}{\partial n} = J_\ell & \text{on the } \ell\text{-th electrode} \\ 0 & \text{elsewhere at the boundary} \end{array} \right] \tag{2}$$

where J_ℓ denotes the current density through the surface of the ℓ-th electrode (Trigo *et al.*, 2004).

In order to solve the Laplace equation, Eq. (1), with boundary conditions, Eq. (2), the closed domain is discretized through the Finite Element Method (FEM), using triangular elements with constant conductivity σ and linear interpolation functions (Murai and Kagawa, 1985). The minimization of the variational principle associated with the Laplace equation provides the local element matrices.

The electrodes are modeled as four-node elements with constant conductance, equally positioned around the border of the discretized domain. The simplified complete model (Hua, Woo, Webster and Tompkins) is used to take into account the high metal conductivity and the skin contact impedance.

When the local element matrices are stated in terms of the global coordinates of the mesh, the global resistivity matrix (Trigo, 2001; Trigo *et al.*, 2004) which includes electrode contact impedance effects, is obtained; then, the following relation holds:

$$YV = C \tag{3}$$

where $Y(\boldsymbol{\sigma}) \in \mathbb{R}^{s \times s}$ is the conductivity matrix calculated at any particular distribution $\boldsymbol{\sigma}_p$, $V(\boldsymbol{\sigma}) = [\boldsymbol{v}_1 ... \boldsymbol{v}_j ... \boldsymbol{v}_p]$, $\boldsymbol{v}_j \in \mathbb{R}^s$ is a matrix containing nodal potentials corresponding to each applied current pattern, and $C = [\boldsymbol{c}_1 ... \boldsymbol{c}_j ... \boldsymbol{c}_p]$, $\boldsymbol{c}_j \in \mathbb{R}^s$ is a matrix of linearly independent bipolar diametrical current patterns (Trigo *et al.*). The superscripts s, m, and ℓ stand respectively for the number of nodes, elements and electrodes of the FE mesh, in which p current patterns are applied.

2.2 Iterated Extended Kalman filter for EIT

A detailed discussion on Kalman filtering theory is out of our current scope. Extensive studies can be found in cited references, such as Gelb (1979), and Jazwinsky (1970). We, however, state the main conditions necessary for applying the filter equations.

Kalman filters demand the description of the dynamical problem in a state-space form, which includes a *system model* and an *observation model*. Several mathematical models in the literature try to describe the phenomena that take place in the cardiovascular system; so far, though, none of them have been able to account for all the effects (gas exchange, thorax movement, cardiac pulsatile characteristic, varying blood and tissue dielectric properties). The same problem occurs in the field of Atmosphere, Ocean and Earch sciences, whose models still poorly represent reality (Burgers, van Leeuwen ans Evensen, 1998). One alternative to circumvent that difficulty is to admit a *random walk* model.

The random walk model compensates for the lack of information on the system itself with the inclusion of a random-noise term. In the case of EIT, the random walk model for the discrete-time evolution of the conductivity $\boldsymbol{\sigma}$ in the medium is (Vauhkonen, Karjalainen and Kaipio, 1998),

$$\boldsymbol{\sigma}_k = \Phi_{k-1}\boldsymbol{\sigma}_{k-1} + \boldsymbol{\omega}_k \,, \tag{4}$$

known as the *state equation*, in which $\Phi_{k-1} \in \mathbb{R}^{m \times m}$ is the discrete-time transition matrix and $\boldsymbol{\omega}_k \in \mathbb{R}^m$ is a zero mean Gaussian white state noise vector whose covariance is the symmetrical positive semi-definite matrix $Q_k \in \mathbb{R}^{m \times m}$. The index k indicates the time-steps $t = k\Delta t$.

The observation model results from the FEM model, as follows: The domain discretization allows the measurement of potential through the electrodes. The measured potentials $\boldsymbol{v}_j$ result from the map $\boldsymbol{h}_j : \boldsymbol{\sigma} \rightarrow \boldsymbol{v}_j$, *i. e.*, the statement of the inverse problem since, from Eq. (3),

$$\boldsymbol{v}_j(\boldsymbol{\sigma}) = \boldsymbol{h}_j(\boldsymbol{\sigma}) = [Y(\boldsymbol{\sigma})]^{-1}\boldsymbol{c}_j, \;\; j = 1, \ldots, p. \tag{5}$$

The discrete-time *nonlinear observation model* is obtained from Eq. (5) by incorporating a noise vector inherent to any measurement process. Thus,

$$\boldsymbol{v}_k(\boldsymbol{\sigma}_k) = \boldsymbol{h}_k(\boldsymbol{\sigma}_\mathbf{k}) + \boldsymbol{\nu}_k, \tag{6}$$

in which $\boldsymbol{\nu}_k \in \mathbb{R}^\ell$ is a zero mean Gaussian white measurement noise vector whose covariance is the symmetrical positive definite matrix $R_k \in \mathbb{R}^{\ell \times \ell}$. The vectors $\boldsymbol{v}_k \in \mathbb{R}^\ell$ and $\boldsymbol{h}_k(\boldsymbol{\sigma}_k) \in \mathbb{R}^\ell$ represent electrode positions on the FE mesh, the only place in which measurements can be made, for each $j = 1 \ldots p$ current pattern.

Linearizing Eq. (6) around the last estimate $\boldsymbol{\sigma}_{k-1} \in \mathbb{R}^m$, and keeping terms up to the first order, results in

$$\boldsymbol{v}_k(\boldsymbol{\sigma}_k) = \boldsymbol{v}_k(\boldsymbol{\sigma}_{k-1}) + \mathbb{H}_k(\boldsymbol{\sigma}_{k-1})\,[\boldsymbol{\sigma}_k - \boldsymbol{\sigma}_{k-1}] + \boldsymbol{\nu}_k, \tag{7}$$

where $\mathbb{H}_k = \frac{\partial \boldsymbol{h}_k}{\partial \boldsymbol{\sigma}}|_{(\boldsymbol{\sigma}_{k-1})} \in \mathbb{R}^{\ell \times m}$ is the *sensitivity matrix* that corresponds to the ℓ potential measurements. The sensitivity matrix is obtained directly from the FE model (Yorkey, Webster and Tompkins, 1987).

Defining a *nominal measurement* (Jazwinski, 1970) as

$$\boldsymbol{z}_k \triangleq \boldsymbol{v}_k(\boldsymbol{\sigma}_k) - \boldsymbol{v}_k(\boldsymbol{\sigma}_{k-1}) + \mathbb{H}_k(\boldsymbol{\sigma}_{k-1})\,[\boldsymbol{\sigma}_{k-1}]\,, \tag{8}$$

and using Eq. (7), one obtains the *linearized observation model* as

$$\boldsymbol{z}_k = \mathbb{H}_k(\boldsymbol{\sigma}_{k-1})\boldsymbol{\sigma}_k + \boldsymbol{\nu}_k \tag{9}$$

Equations (4) and (9) define the state-space representation of the system, and the iterated extended Kalman filter can be readily implemented. We point out that, throughout this work, it is assumed that the process noise and the measurement noise are not correlated, i.e. $\mathcal{E}[\boldsymbol{\omega}_k\boldsymbol{\nu}_k^T] = 0$ for all k, and that both process and measurement noise covariance matrices are diagonal with equal and constant elements, or $Q_k = \rho_\omega^2 I_m$ and $R_k = \rho_\nu^2 I_\ell$, with ρ_ω^2 and ρ_ν^2 representing respectively process and measurement noise covariances. Those hypotheses are used for the sole purpose of simplifying the calculations involved in the iterative procedure.

The iterated extended Kalman filter differs from the extended version in the sense that the linearized observation model of Eq. (9) is obtained thru repeatedly linearizing Eq. (6) around the last estimated state; thus, new estimates are re-calculated using the same measurement vector $\boldsymbol{v}_k$ until there is no significative discrepancy between two consecutive estimated states. There are several forms to present the filter equations; the one below is based in Gelb (1979) and Jazwinski (1970), as follows:

$$\hat{\boldsymbol{\sigma}}_k^{(-)} = \Phi_{k-1}\hat{\boldsymbol{\sigma}}_{k-1}^{(+)} \tag{10}$$

$$P_k^{(-)} = \Phi_{k-1}P_{k-1}^{(+)}\Phi_{k-1}^T + Q_{k-1} \tag{11}$$

Equations (10) and (11) represent the so called *propagation stage*[1]. When new measured data are available, the *update stage* calculates the Kalman gain G_k and corrects the propagated state, $\hat{\boldsymbol{\sigma}}_k^{(-)}$, and error covariance matrix, $P_k^{(-)}$, through equations

$$\hat{\boldsymbol{\sigma}}_{k,j+1}^{(+)} = \hat{\boldsymbol{\sigma}}_k^{(-)} + G_{k,j}\left\{\boldsymbol{v}_k - \boldsymbol{h}_k(\hat{\boldsymbol{\sigma}}_{k,j}^{(+)}) + \mathbb{H}(\hat{\boldsymbol{\sigma}}_{k,j}^{(+)})\left[\hat{\boldsymbol{\sigma}}_k^{(-)} - \hat{\boldsymbol{\sigma}}_{k,j}^{(+)}\right]\right\} \tag{12}$$

$$G_{k,j} = P_k^{(-)}\mathbb{H}_k^T(\hat{\boldsymbol{\sigma}}_{k,j}^{(+)})\left[\mathbb{H}_k(\hat{\boldsymbol{\sigma}}_{k,j}^{(+)})P_k^{(-)}\mathbb{H}_k^T(\hat{\boldsymbol{\sigma}}_{k,j}^{(+)}) + R_k\right]^{-1} \tag{13}$$

$$P_{k,j+1}^{(+)} = \left[I - G_{k,j}\mathbb{H}_k^T(\hat{\boldsymbol{\sigma}}_{k,j}^{(+)})\right]P_k^{(-)}, \tag{14}$$

that re-calculate the state and the error covariance matrix until

$$\|\hat{\boldsymbol{\sigma}}_{k,j}^{(+)} - \hat{\boldsymbol{\sigma}}_{k,j-1}^{(+)}\|_{\mathfrak{p}} \leq \delta, \tag{15}$$

where $\|\cdot\|$ is a $\mathfrak{p}$-order norm and δ is empirically chosen. In this work, we use the Euclidean norm as the evaluation parameter. The iterative estimation process can start as soon as initial state $\boldsymbol{\sigma}_0$, and covariance matrices P_0, Q_0 and R_0 are provided.

2.3 Adaptive State Noise Estimation

An important drawback for the implementation of Kalman filters in EIT is the arbitrary choice of the state noise covariance matrix Q, once little is known about the real system dynamics. Normally, this matrix is kept constant during the whole estimation process. Nevertheless, as is known in Kalman filter theory (Jazwinski, 1970), Q matrix exerts a key influence upon state estimates and, consequently, upon the convergence of the process.

The *adaptive state noise estimation technique* uses information provided by the filter itself in order to modify Q_k and prevent eventual divergence.

Kalman filter divergence is ascertained when the statistics of the *observation residuals* (the difference between the real measured value and the value calculated by the filter using the last available state estimate) are inconsistent with their expected values (Rios Neto and Kuga, 1985). In practical terms, convergence is verified through *normalized observation residuals*, defined as

$$r_\nu \triangleq \left\{\frac{1}{\ell}\sum_{j=1}^{\ell}[\boldsymbol{v}_k(\boldsymbol{\sigma}_k) - \hat{\boldsymbol{v}}_k(\hat{\boldsymbol{\sigma}}_k)]_j\right\}/\zeta_\nu, \quad k = 1, 2, \ldots, \tag{16}$$

[1]The symbol "∧" indicates an *estimate*, while the superscripts "(-)" and "(+)" stand respectively for "immediately before" and "immediately after" arrival of a new batch of measurements.

with ℓ and ζ_ν respectively stating the number of measurements and the standard-deviation of the measurement noise. If

$$\mathbb{E}[r_\nu] = 0 \quad \text{and} \tag{17}$$

$$-3\zeta_\nu \leq r_\nu \leq 3\zeta_\nu, \tag{18}$$

during the whole estimation procedure, convergence is considered satisfactory (Fleury, 1985). The adaptive state noise technique, presented in Jazwinski (1970), seeks to *adapt* the state noise covariance matrix so as to maximize the probability that the observed and expected residual statistics are consistent. This approach does not consider the fact that the residuals incorporate the uncertainty associated to the sensor, through measurement noise covariance matrix R.

Another approach, that excludes the influence of measurement noise from the above-cited maximization problem, was proposed by Rios Neto and Kuga (1985). This method aims at obtaining a diagonal matrix $Q_{d_{k-1}} \in \mathbb{R}^{m\times m}$, with main diagonal $\boldsymbol{q}_k \geq \mathbf{0} \in \mathbb{R}^m$, that promotes consistency between observed and expected statistics of the residuals. The main idea is to describe the problem of obtaining $Q_{d_{k-1}}$ as a state-space problem, using $\boldsymbol{q}_k$ as the state-vector and a random-walk model for its dynamics, besides an auxiliary Kalman filter to predict the state.

An observation model with *pseudo-measurements* to be used with the auxiliary Kalman filter is built from observed residuals and the sensitivity matrix of the main inverse-problem. The state and observation equations for the auxiliary Kalman filter are (Rios Neto and Kuga, 1985)

$$\boldsymbol{q}_{k+1} = \boldsymbol{q}_k + \boldsymbol{\varsigma}_k. \quad \text{and} \tag{19}$$

$$\boldsymbol{v}_k^p = (\mathbb{H}_k^p)\boldsymbol{q}_k + \boldsymbol{\eta}_k, \tag{20}$$

with $p \triangleq$*pseudo* and $\boldsymbol{v}_k^p \in \mathbb{R}^m$ the pseudo-measurement. Vector $\boldsymbol{\varsigma}_k \in \mathbb{R}^m$ is zero-mean Gaussian with covariance

$$\mathbb{E}[\boldsymbol{\varsigma}_i\boldsymbol{\varsigma}_j^T] = \begin{cases} Q_{d_i^p} & \text{if } i = j \\ 0 & \text{if } i \neq j \end{cases} \tag{21}$$

Vector $\boldsymbol{\eta}_k \in \mathbb{R}^m$ is a zero-mean noise vector such that

$$\mathbb{E}[(\boldsymbol{\eta}_k)_j^2] = 4[(\boldsymbol{v}_k(\boldsymbol{\sigma}_k) - \hat{\boldsymbol{v}}_k(\hat{\boldsymbol{\sigma}}_k))_j^r]^2 (R_k)_{jj} + 2(R_k)_{jj}^2. \tag{22}$$

The subscript jj indicates each element of the measurement noise covariance matrix diagonal, whereas the pseudo-sensitivity matrix $\mathbb{H}_k^p$ and the sensitivity matrix of the original observation model comply with

$$(\mathbb{H}_k^p)_j \boldsymbol{q}_k = (\mathbb{H}_k)_j Q_{dk-1}[(\mathbb{H}_k)_j]^T \tag{23}$$

Estimates of the adaptive-noise vector $\boldsymbol{q}_k$ according to Eqs. (19) and (20) are obtained through a conventional Kalman filter and used by the main filter, the iterated extended in our case.

2.4 Two-phase Identification Procedure

A two-phase identification procedure that separates the problems of estimating medium conductivity distribution and medium-electrode contact impedances was proposed and evaluated by Trigo *et al.* (2004). The first phase concerns the estimation of electrode contact impedances while keeping the medium conductivity distribution constant. On the second phase, the previously estimated electrode impedances remain constant while the Kalman filter provides estimates for the medium conductivity distribution. Phases one and two are alternately applied until the convergence criteria are fulfilled. The reasoning behing this approach is based on the *Contraction Mapping Theorem*.

Kalman filter can be understood as a recursive least-squares minimization procedure (Jazwinski, 1970) that, at each iteration, contracts the error covariance matrix trace. If one admits that, in a metric space $\mathbb{S}$, the Kalman filter converges in a neighbourhood of $\boldsymbol{\sigma_0} \in \mathbb{S}$ (initial estimate) of radius r, to a vector $\hat{\boldsymbol{\sigma}}^*$ (Holtzman, 1970), when the trace of P_k is chosen as the norm for the space $\mathbb{S}$, each iteration on subspaces $\mathbb{S}_M$ (M means "medium"), or $\mathbb{S}_E$ (E means "electrodes"), of $\mathbb{S}$, represents a contraction within this space. The sequential contractions on those subspaces or the repetition of contractions within one subspace will lead to an estimate that also lies in the r-vicinity of $\boldsymbol{\sigma_0}$, according to the Contraction Mapping Theorem.

3. Methods

The experimental validation of the models developed was performed using a $235\ mm$-diameter cylindrical phantom with 32 rectangular $12\ mm$-wide brass electrodes placed around the container's border, keeping an equal gap between each other. The container was filled with a $NaCl$ solution of concentration 0,23 g/l up to a $26,5mm$ height. Bipolar diametrical current patterns with frequency $25\ kHz$ and amplitude $2mA$ peak-to-peak were injected by a current mirror

type generator, as described in Bertemes-Filho, Brown and Wilson (2001). A multimeter HP 34401A was used to measure potentials at the electrodes (Trigo, 2001; Trigo *et al.*, 2004). A $62\ mm$-diameter cylindrical glass object is immersed in the homogeneous medium, representing a step-function perturbation. We stress that neither the conductivity of this object nor the conductivity distribution of the saline solution are known *a priori*.

The phantom is represented by a circular domain, which is discretized by the FEM, as seen on Fig. 1, in $m = 272$ elements, from which $\ell = 32$ elements have four nodes; the total number of nodes is $s = 201$. The 32 elements with four nodes represent electrodes, modeled using the simplified complete model (Hua, Woo, Webster and Tompkins, 1993).

The iterated extended Kalman filter with adaptive state noise is used to estimate electrode contact impedances, and to identify the position of the glass object, in two phases, as described in section 2.4 The 240 elements that comprise the medium are grouped in 32 ROIs (Trigo, 2001), according to Fig. 1. The identification of the resistivities on those regions is one of the phases; the other refers to the identification of the 32 impedances at the interfaces between the saline medium and the metallic surface of the electrodes.

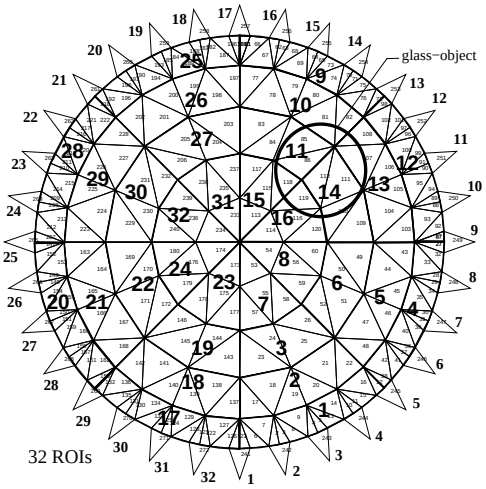

Figure 1. 272-element mesh with 32 ROIs

The initial parameters used on the identification procedure are presented in Table 1.

Table 1. Initial parameters for phases 1 and 2

identification sequence				P_0	Q	R
nr.	phase	δ	iterations			
1	1 (electrode)	0,30	96	$3,5 \times 10^{-4} I_{32}$	$7,8 \times 10^{-4} I_{32}$	$2,5 \times 10^{-3} I_{32}$
2	2 (medium)	0,30	96	$3,5 \times 10^{-1} I_{32}$	$7,8 \times 10^{-3} I_{32}$	$2,5 \times 10^{-3} I_{32}$
3	1 (electrode)	0,30	96	$3,5 \times 10^{-4} I_{32}$	P_{32}	$2,5 \times 10^{-4} I_{32}$
4	2 (medium)	0,30	320	$3,5 \times 10^{-1} I_{32}$	$0,4 \times P_{32}$	$2,5 \times 10^{-4} I_{32}$
4a	2 (medium)	0,30	320	$3,5 \times 10^{-1} I_{32}$	$0,4 \times P_{32}$	$2,5 \times 10^{-4} I_{32}$
5	1 (electrode)	0,80	96	$3,5 \times 10^{-4} I_{32}$	$0,4 \times P_{32}$	$2,5 \times 10^{-4} I_{32}$
6	2 (medium)	0,20	96	$3,5 \times 10^{-1} I_{32}$	$0,4 \times P_{32}$	$2,5 \times 10^{-4} I_{32}$
6a	2 (medium)	0,36	96	$3,5 \times 10^{-1} I_{32}$	$0,4 \times P_{32}$	$2,5 \times 10^{-4} I_{32}$

4. Results

Table 2 states electrode contact impedances obtained after identification sequences 1, 3 and 5, phase 1. The mean value is $0,014\ (\Omega \cdot m^2)$, and the standard deviation is $0,006\ (\Omega \cdot m^2)$. Figure 4(a) shows a 3D-plot of the last-iteration estimated medium resistivity distribution for identification sequence 6a, phase 2, whereas Fig. 4(b) presents its normalized residual time-history.

5. Discussion

According to the Contraction Mapping Theorem, electrode contact impedances shown on Tab. 2 represent the partial state estimated on phase 1, which lies on the subspace $\mathbb{S}_E$. Supposing that the resistivity distribution estimated on phase 2 belongs to the subspace $\mathbb{S}_M$, the estimation procedure, as a whole, should converge to a state in the neighbourhood of

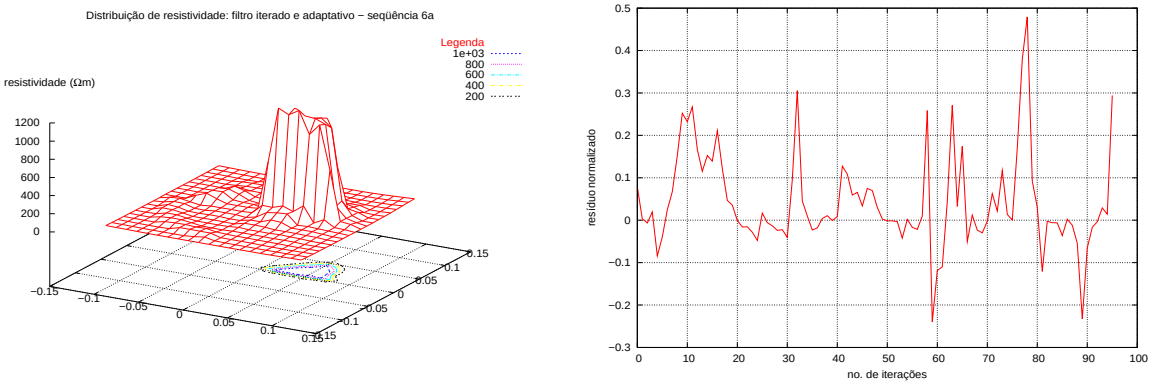

(a) last state estimated by the filter

(b) normalized residual

Figure 2. Results of identification sequence 6a

Table 2. Electrode contact impedances $(\Omega \cdot m^2)$

ELECTRODE	1	2	3	4	5	6	7	8
IMPEDANCE	0,0099	0,0141	0,0078	0,0105	0,0212	0,0270	0,0133	0,0181
ELECTRODE	9	10	11	12	13	14	15	16
IMPEDANCE	0,0259	0,01167	0,0139	0,0136	0,0090	0,0141	0,0067	0,0098
ELECTRODE	17	18	19	20	21	22	23	24
IMPEDANCE	0,0158	0,0145	0,0157	0,0105	0,0253	0,0187	0,0070	0,0085
ELECTRODE	25	26	27	28	29	30	31	32
IMPEDANCE	0,0104	0,0098	0,0093	0,0164	0,0168	0,0133	0,01301	0,0058

the true state.

These hypotheses are corroborated by the behaviour of normalized residuals, Fig. 4(b), whose actual statistics (mean value=$0,042$, standard deviation=$0,11$) are consistent with their expected values, thus complying with criteria stated on Eqs. (17) and (18), and assuring convergence of the process as a whole. The glass-object of unknown resistivity was properly identified on phase 2, without any *a priori* information on its true position. Besides that, the ROIs we use have no resemblance with the shape of the object. Therefore, the identification process can be considered general.

It must be pointed out that the convergence of the process is slow. The number of iterations shown on Tab. 1 express how many times the iterated Kalman filter changed from a *local iteration* (Jazwinski, 1970) to a global iteration. Perhaps one reason for the reduced convergence speed is the high amplitude of the step-function perturbation, which forces the filter to track the change with little information (only 32 potentials are used to estimate 272 parameters), a feature of the ill-posed inverse problem.

6. Conclusion

This work has investigated the application of the iterated extended Kalman filter incorporating adaptive noise techniques, to track impedance changes in EIT. A two-phase estimation procedure was used. Results with experimental data from a phantom indicate that the the proposed approach can be employed on medical applications whose main concern is accurateness of the estimated images. Convergence was accomplished according to statistical criteria, which is a novelty presented in this paper. Although convergence is still slow, the method can be improved by parallel computation and sparse matrix techniques. In addition, implementations of the method using other system models should be investigated.

7. References

Barber, D.C. and Brown, B.H., 1984, "Applied potential tomography", J. Phys. E: Sci. Instrum., Vol. 17, pp. 723-733.

Bertemes-Filho, P., Brown, B.H., and Wilson, A.J., 2001, "A comparison of modified Howland circuits as current generators with current mirror type circuits", Physiol. Meas., Vol. 21, pp. 1-6.

Burgers, G., van Leeuwen, P.J., and Evensen, G., 1998, "Analysis Scheme in the ensemble Kalman Filter", Monthly Weather Rev., Vol. 126, pp. 1719-1724.

Fleury, A.T., 1985, "Estimadores de Estado de Sistemas Dinâmicos Baseados no Conceito de Dualidade", Tese de Doutorado, EPUSP, São Paulo, Brazil.

Gelb, A. (Editor), 1979, “Applied Optimal Estimation”, MIT Press, Cambridge, USA, 382 p.

Holtzman, J.M., 1970, “Nonlinear System Theory - A Functional Analysis Approach”, Prentice-Hall, New York, USA, 213 p.

Hua,P., Woo, E.J., Webster, J.G., and Tompkins, W.J., 1993, “Finite Element Modeling of Electrode-Skin Contact Impedance in Electrical Impedance Tomography”, IEEE Transactions on Biomedical Engineering, Vol. 40-4, pp. 335-343.

Jazwinski, A.H., 1970, “Stochastic Processes and Filtering Theory”, Academic Press, New York, USA, 376 p.

Kim, K.Y., Kang, S.I., Kim, M.C., Lee, Y.J., and Vauhkonen, M., 2002, “Dynamic Image Reconstruction in Electrical Impedance Tomography With Known Internal Structures”, IEEE Transactions on Magnetics, Vol. 38-2, pp. 1301-1304.

Kim, K.Y., Kim, B.S., Kim, M.C., Lee, Y. J., and Vauhkonen, M., 2001, “Image reconstruction in time-varying electrical impedance tomography based on the extended Kalman filter”, Measurement Science and Technology, Vol. 12, pp. 1032-1039.

Murai, T., Kagawa, Y., 1985, “Electrical Impedance Computed Tomography Based on a Finite Element Model”, IEEE Transactions on Biomedical Engineering, Vol. 32-3, pp. 177-184.

Rios Neto, A., and Kuga, H.K., 1985, “Kalman filtering state noise adaptive estimation”, Annals of the ELECOM’85, Rio de Janeiro, Brazil.

Trigo, F.C., 2001, “Filtro Estendido de Kalman Aplicado à Tomografia por Impedância Elétrica”, Dissertação de Mestrado, EPUSP, São Paulo, Brazil.

Trigo, F.C., González-Lima, R., and Amato, M.B.P., 2004, “Electrical impedance tomography using the extended Kalman Filter, IEEE Transactions on Biomedical Engineering”, Vol 51-1, pp. 72-81.

Vauhkonen, M., Karjalainen, P.A., and Kaipio, J.P., 1998, “A Kalman Filter Approach to Track Fast Impedance Changes in Electrical Impedance Tomography”, IEEE Transactions on Biomedical Engineering, Vol. 45-4, pp. 486-493.

Yorkey, T.J., Webster, J.G., Tompkins, W.J., 1987, “Comparing Reconstruction Algorithms for Electrical Impedance Tomography”, IEEE Transactions on Biomedical Engineering, Vol. 34-11, pp. 843-852.